Supplementary Information

Targeted drug delivery and image-guided therapy of heterogeneous ovarian cancer using HER2-targeted theranostic nanoparticles

M. Satpathy *et al*.

Figure S1. Determination of effect of the level of HER2 expression in human ovarian cancer cells on response to theranostic IONP treatment *in vitro*.

The effect of NIR-830-$Z_{HER2:342}$-IONP-Cisplatin was examined in HER2 high SKOV3-luc cells and HER2 low OVCAR3 cell lines. Cells were seeded in a 96-well plate overnight and equivalent concentration of cisplatin (5 μM) of different treatment IONPs were then added to the cells for 72 hours. No treatment group served as a control (100%). Alamar blue cell proliferation assay was used. Fluorescent intensity (Excitation/Emission: 560/585 nm) was measured using a microplate reader (SpectraMAX Plus 384, Molecular Devices, Sunnyvale, CA, USA). Cell viability assay determined cytotoxicity of different cisplatin formulations in HER2 high (SKOV3-luc) and HER2 low (OVCAR3) tumor cells 72 hours following treatment. Student's *t*-test: *p<0.01, **p<0.05, ***p<0.005, n=4.

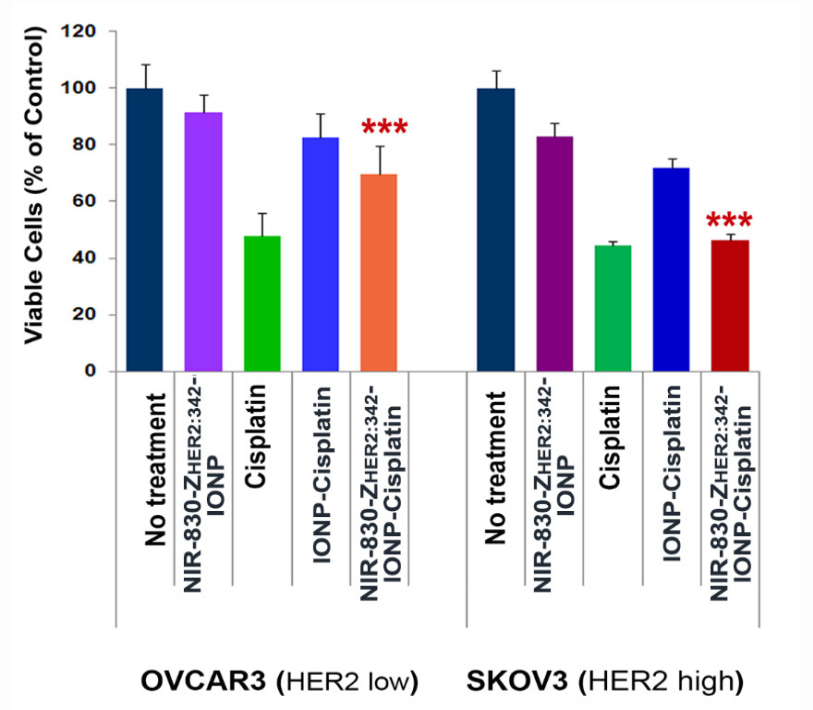

Figure S2 Determination of targeted delivery of NIR-830-$Z_{HER2:342}$–IONP *in vivo* by whole body and *ex vivo* optical imaging, chemical and histological analyses.

(A) Optical imaging at 48 hours following one i.v. injection of 190 picomolar (pmol) of NIR-830-$Z_{HER2:342}$–IONP showed strong optical signals in the primary tumor (pink arrow) and lung metastatic tumor (yellow arrow). Result of the second optical imaging performed after the second i.v. injection of 400 pmol of the above IONPs in the same mouse is shown in Figure 2E. Numbers: tumor signal to body background ratio. (**B)** Histological confirmation of targeted delivery into the primary tumor (upper) and lung metastases (middle) by Prussian blue staining on tumor tissue (upper panel) and micrometastases in the lung (middle panel). NIR-830-BSA–IONP was not found in primary tumor tissues (bottom). (**C**) Determination of biodistribution of NIR-830-$Z_{HER2:342}$–

IONP-Cisplatin and targeted IONP-Cisplatin by chemical analysis of iron contents in tumor and normal tissue lysates. Tumor and normal tissue lysates collected at 48 h following nanoparticle delivery were analyzed by chemical analysis (color metric Prussian blue solution) for iron concentration, which represented the amount of IONP accumulation. Based on the iron concentration and tumor weight, we estimated that the percentage of total delivered dose in the tumor obtained from the mouse treated with NIR-830-$Z_{HER2:342}$–IONP-Cisplatin was 13.5%. Similar analysis showed that the percentage of non- targeted IONP-Cisplatin that was accumulated in the tumor tissue was 3%. The spleen had the highest level of iron, which was the results of a high level of pre-existing iron and non-specific uptake by macrophages. The level of iron in the liver was slightly higher compared to the tumor tissue.

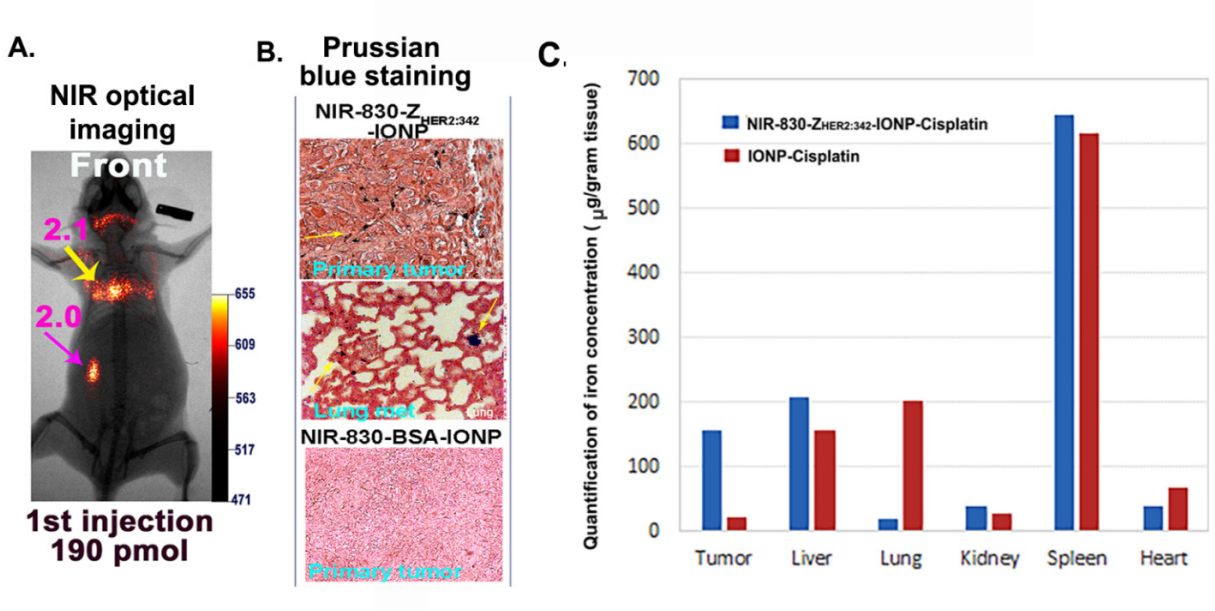

Figure S3. Therapeutic response of primary and metastatic tumors following treatment with low cisplatin equivalent doses of the targeted IONP-Cisplatin in the orthotopic ovarian cancer model.

Treatment of the tumor bearing mice with low cisplatin doses should provide the information about tumor response when the level of drug delivery is low. Following six treatments with a very low dose (0.5 mg/kg) of the targeted-IONP-Cisplatin, we observed 40% of inhibition of the tumor volume, while unconjugated cisplatin failed to produce apparent anti-tumor effect. Even at this low dose, we observed 76% of growth inhibition of the peritoneal metastases, while only 7% of tumor growth inhibition was seen in the primary tumor (Upper panel). The mean tumor weights of total visible tumors as well as primary, or i.p. metastatic tumors are shown. n=4-5 mice/group. Student's *t*-test: no treatment control vs targeted-IONP-Cisplatin: metastases: $p = 0.03$. There was no statistical significant difference among other groups. Additionally, therapeutic response rendered by the targeted-IONP-Cisplatin at 2 mg/kg dose exhibited 67% inhibition of total tumors while unconjugated cisplatin inhibited 44% of tumor growth (lower panel). However, due to the presence of a wide range of tumor responses among different mice within the same group, there was no statistical significant difference of the tumor weights among the different mouse groups treated with 2 mg/kg cisplatin equivalent dose.

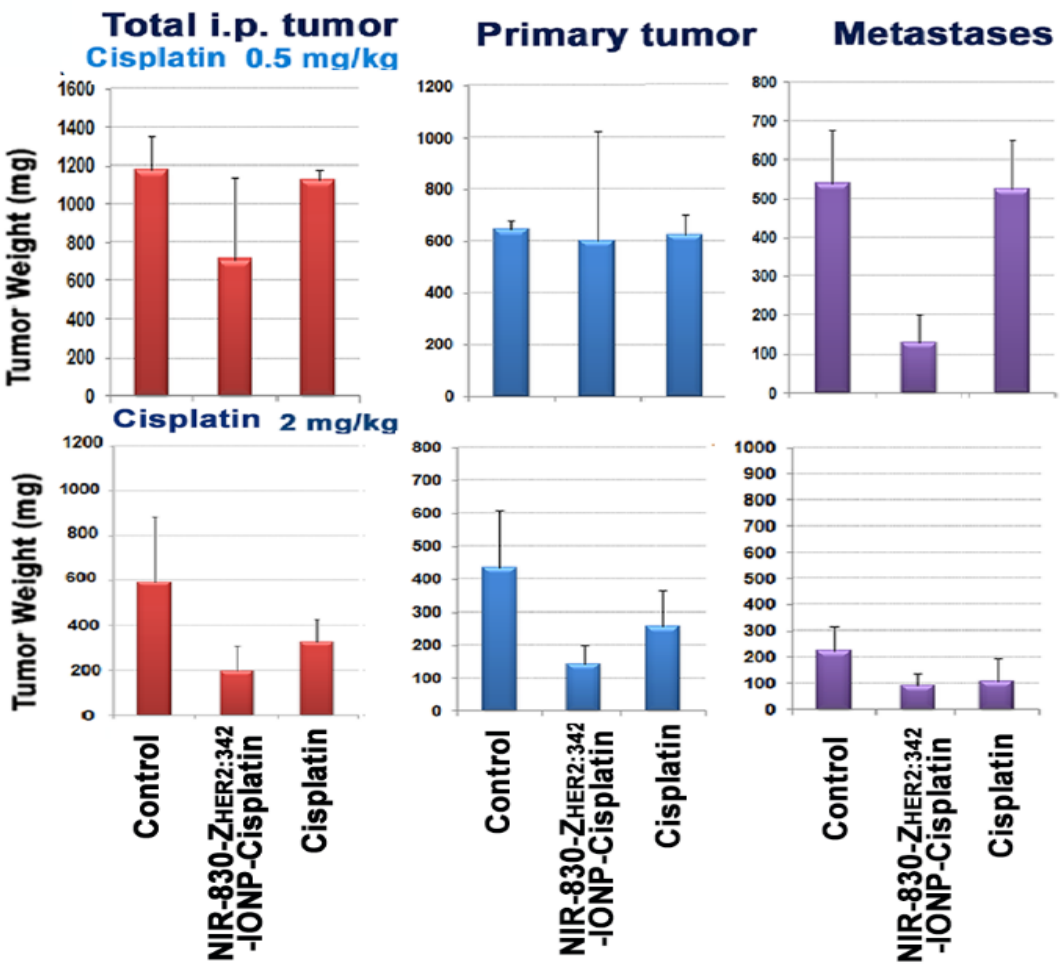

Figure S4. Histological and chemical analyses of tumor tissues collected from no treatment control and theranostic IONP treated mice.

(A) H&E staining showed that no treatment, cisplatin, non-targeted-IONP-Cisplatin treated tumors had dense tumor cells. However, residual primary tumors collected from NIR-830-$Z_{HER2:342}$-IONP-Cisplatin treated mice showed heterogeneous responses. Many had small tumors with large necrotic areas (red arrows). A poorer responder tumor had remaining tumor cell clusters (green arrows) near a normal follicles (blue arrow). Cis. Cisplatin. (**B**) Platinum (Pt) concentrations in tumors were measured using a modified platinum colorimetric assay. Tumor tissues obtained from mice treated with non-targeted or targeted IONP-Cisplatin had 2- to 3-fold higher Pt than that of unconjugated cisplatin and 7- to 8-fold higher Pt concentration than the no-treatment control. Although platinum concentration in NIR-830-$Z_{HER2:342}$-IONP-Cisplatin-treated tumor was only slightly higher than that of non-targeted IONP-Cisplatin, the level of Pt in the tumors after completing the therapy was likely the result of both intratumoral delivery and the presence of drug-resistant tumor cells with nanoparticle-drug conjugate. It is likely that drug-sensitive tumor cells were killed and disintegrated and therefore, lost nanoparticle-drug, while the resistant tumor cells survived and retained the nanoparticle-drug for longer time. The bar figure shows the mean Pt concentration (μg/mg of tissue) in each treatment group. Three samples were examined in each group.

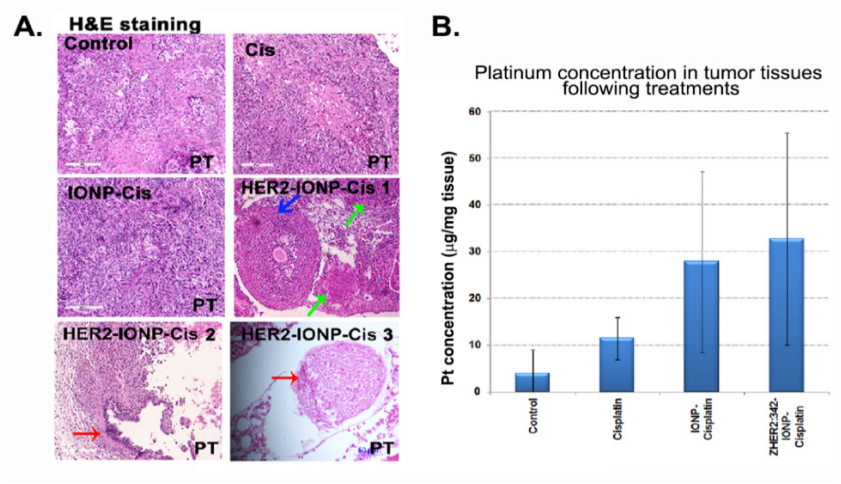

Figure S5. Evaluation of systemic toxicity of NIR-830-$Z_{HER2:342}$-IONP-Cisplatin in tumor bearing mice following targeted therapy.

Serum samples were collected five days following the last treatment of a 5 mg/kg cisplatin equivalent dose for serological analysis of liver and kidney function. There was no significant difference among the control groups and targeted nanoparticle drug delivery group in the levels of aspartate aminotransferase (AST) and alanine aminotransferase (ALT). The level of ALT was lower in the targeted therapy group compared to the non-treatment control. The mean level of ALT or AST of each group (light blue bar) and the level of individual mice (n=6) are shown. The level of serum creatinine, an indicator of kidney function, was normal (≤0.2 mg/dl) in all mouse groups. It is likely that massive growth of peritoneal tumors and the presence of ascites in the no treatment mice led to abnormal liver function while the mice that received the targeted therapy had normal liver function due to smaller primary tumors and a fewer i.p. metastases. Body weight of the mice were recorded from different groups (n=5 mice/group). There was no body weight decrease in the mice received targeted theranostic IONP-Cisplatin. Day 0: treatment started and Day 36: mice were sacrificed. No-treatment control mice had slightly increased body weight due to the presence of ascites in some mice. Although there was no significant serological change, the survival mice treated with 5 mg/kg of unconjugated cisplatin had noticeable side effects, such as weight loss and death of one of five mice in the group.

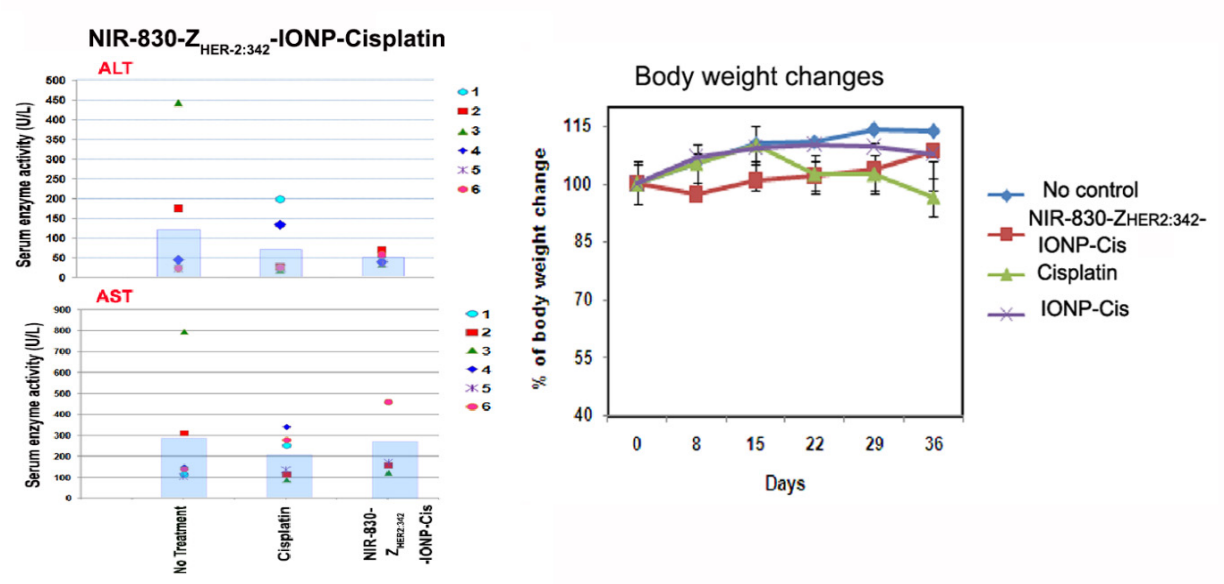

Figure S6. Histological examination of systemic toxicity in normal organs collected from mice that received different treatments by H&E staining.

Frozen tissue sections of normal organs in the mice that received the targeted or non-targeted theranostic-IONP-Cisplatin (5 mg/kg cisplatin dose) had normal morphology. However, treatment with the same dose of unconjugated cisplatin led to abnormal morphology and necrotic areas in the liver, spleen, and kidney (yellow arrows).

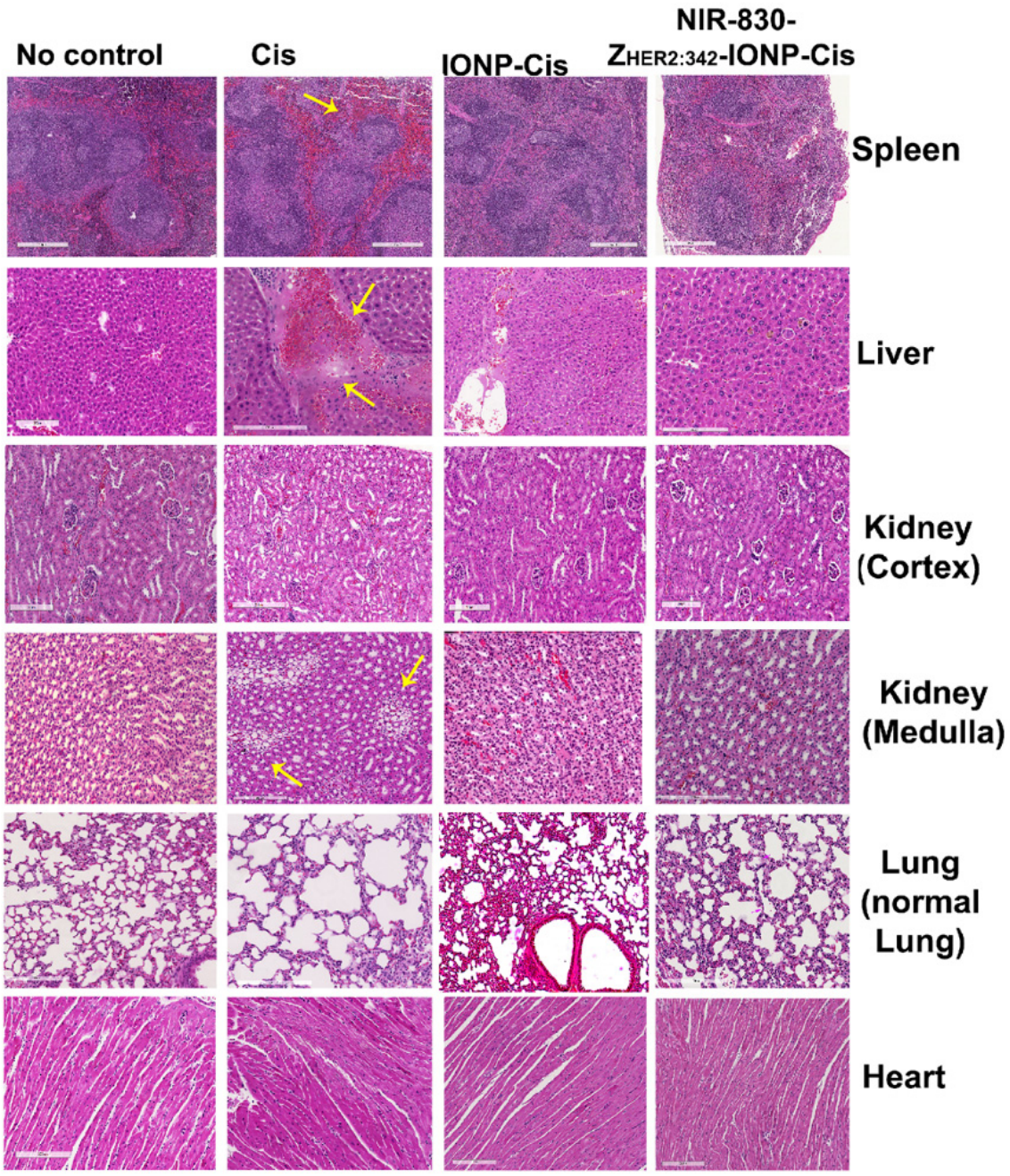

Figure S7. Bioluminescence and MR imaging for detection of the effect of HER-2 targeted therapy in the orthotopic ovarian cancer xenograft model.

Tumor bearing mice received equal iron concentration of IONPs (non-targeting), IONP-Cisplatin (non-targeting), and NIR-830-$Z_{HER2:342}$-IONP-Cisplatin (5 mg/kg of cisplatin equivalent dose) for six treatments. BLI and T_2-weighted MR imaging (3T MRI scanner) were conducted on the mice. Mice treated with IONP-only had a large primary tumor (pink) and i.p. metastases (yellow). IONP-Cisplatin treated mice had large primary tumors without detectable metastases. Mice treated with targeted theranostic IONP-Cisplatin had small primary tumors and no detectable metastases. T_2-weighted MR images revealed a small tumor lesion below the kidney (pink arrow) that had a significant T_2 signal intensity decrease (28%) compared to tumors in the other two control mice (p<0.005). Large primary and metastatic tumor lesions in the IONP-only treated mice had high levels of T_2 signal intensity and were visible in the MR image (pink circled areas). Pink numbers: Mean relative MRI T_2 signal intensity of the entire tumor slices.

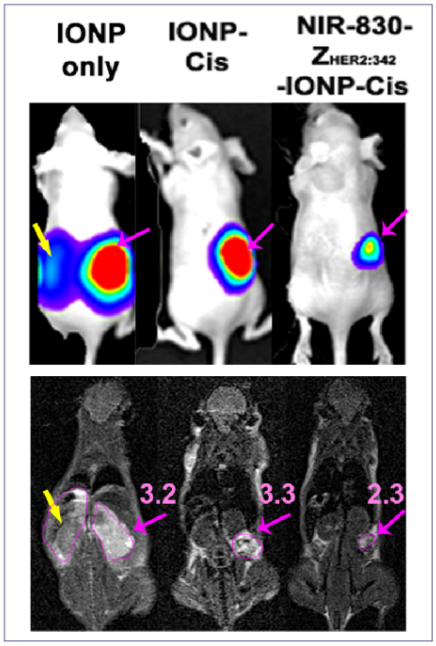

Figure S8. Quantification of lung metastatic lesions by H&E staining.

H&E stained paraffin lung tissue sections were examined under a bright field microscope and the presence of tumor nodules was recorded. The bar graph shows the mean number of lung metastases with standard deviation in four mouse groups. There was a siginificant inhibition of the decvelopment of lung metastases in mice that received NIR-830-$Z_{HER2:342}$-IONP-Cisplatin treatment compared to no treatment control (Student's t-test, p=0.05, n=6). There was no statistically significance among the others groups (p> 0.05).

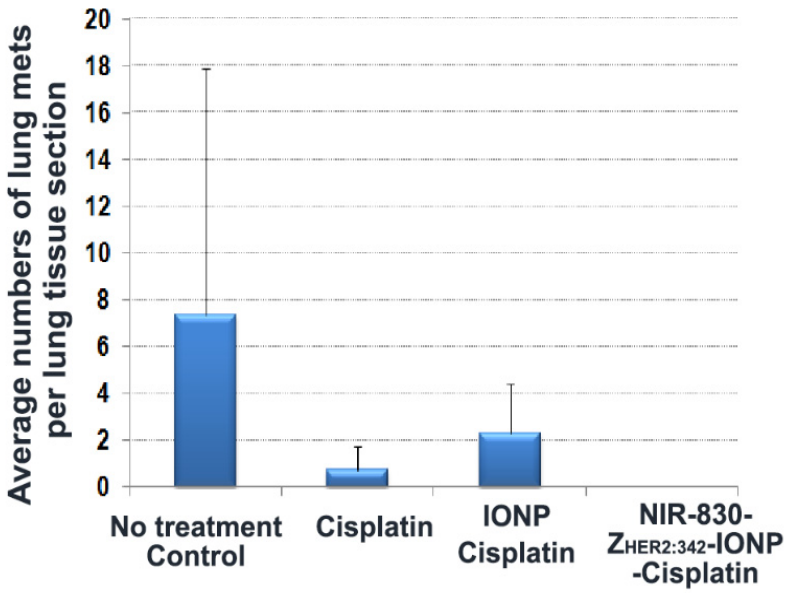

Figure S9. Spectroscopic intraoperative imaging system and detection of dual imaging signals in drug resistant residual tumors.

(**A**) Schematic illustration of a custom built handheld spectroscopic imaging device that can be used as an intraoperative imaging device (50). This device has a compact 1x10 cm probe connected to a 5-meter fiber optic cable for both laser excitation and efficient light collection. The excitation source is a 785 nm diode laser with a focal spot of 0.1 to 1 mm. It covers spectral ranges of 250-2000 cm^{-1} at better than 10 cm^{-1} resolution, corresponding to a wavelength of 800-930 nm with a 0.6 nm resolution. An attached spectrometer and laptop computer can instantly acquire and analyze spectral data in 1-2 seconds. To monitor the entire surgical area, the spectroscopic imaging device is integrated with a wide-field color imaging system. There are three optical channels that are separated using dichroic beam-splitters: (**i**) a spectroscopic channel, (**ii**) a laser line channel, and (**iii**) a standard color video channel. Signals in these three channels are processed by a computer and co-displayed on a color monitor. (**B**) Detection of dual spectroscopic and NIR signals in drug resistant tumor lesions in the peritoneal cavity following targeted therapy using NIR-830-$Z_{HER2:342}$-IONP-Cisplatin. Strong spectroscopic imaging signals were detected in the small metastatic tumor nodules in the peritoneal cavity, such as tumors on the mesentery and fallopian tubes (blue arrows). However, normal mesentery and muscle areas did not have detectable signals (white arrows). **C**. Quantification of biodistribution of NIR-830-$Z_{HER2:342}$-IONP-Cisplatin using spectroscopic imaging following systemic administration. After targeted therapy, mice were sacrificed, and tissues were harvested for examination of spectroscopic signal intensity *ex vivo*. In normal organs, the lung, heart and muscle had the lowest signal while kidneys had the highest signal. Tumors had the second highest level of spectroscopic signals in both mice, which were 4.5 to 8 fold higher than that detected in muscle. In those mice, tumor signals were higher than that in the liver.

A. Spectroscopic imaging system

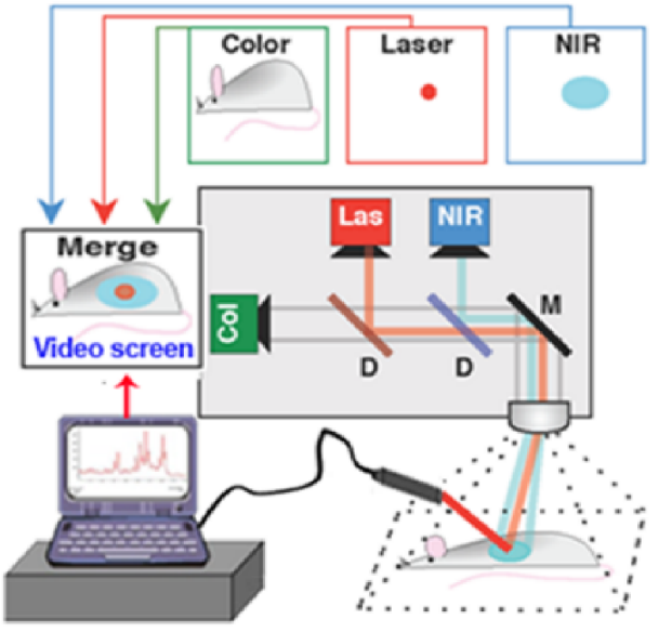

B. Spectroscopic detection of i.p. tumors

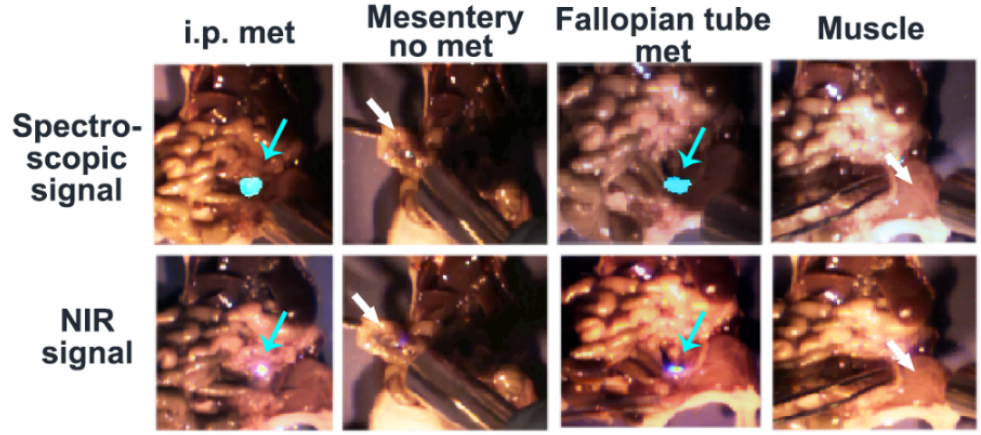

C. Ex vivo detection of spectroscopic signal